https://doi.org/10.3311/PPci.21006
Creative Commons Attribution


**Periodica Polytechnica Civil Engineering,** 67(2), pp. 571–581, 2023

# Study of the Key Mechanical Properties of Welded Hollow Spherical Joints after Uniform Corrosion

Feng Qiu[1], Yinsong Wang[2*], Yu Gao[2], Zhiwei Zhan[g1,2], Hongliang Qian[1,2], Huajie Wang[1,2], Feng Fan[1]

[1] School of Civil Engineering, Harbin Institute of Technology, 150090, Harbin, Heilongjiang, China
[2] Department of Civil Engineering, Harbin Institute of Technology at Weihai, 264209, Weihai, Shandong, China
[*] Corresponding author, e-mail: 21S130395@stu.hit.edu.cn

Received: 15 August 2022, Accepted: 20 February 2023, Published online: 28 February 2023

**Abstract**

The welded hollow spherical joint is the most common form of the spatial grid structure, but the corrosion treatment at the joint is difficult. There are many corrosion problems of the welded hollow spherical joint in the actual structure, which brings hidden problems to structural safety. To study the effects of uniform corrosion on the key mechanical properties of welded hollow spherical joints, the joint refinement FEM in one typical size is built considering the effect of uniform corrosion through the method of the element birth and death, and the tensile, compressive, and bending performance of the FEM has been analyzed. Based on the analysis results, the relation curves between the three bearing capacities of the welded hollow spherical joint and the uniform corrosion degree are given. The results show that the influence of early corrosion on the joint tensile and compressive performance is not obvious. After corrosion to a certain extent, the loss of tensile and compressive capacity has a significant linear relationship with the degree of corrosion, and the loss of bending capacity has a significant quadratic curve relationship with the degree of corrosion from the initial stage. This study can provide a theoretical reference for a better understanding of the mechanical properties of welded hollow spherical joints in one typical size after corrosion to evaluate structural safety.

**Keywords**

spherical joint, uniform corrosion, birth-death element, degradation of bearing capacity, failure mode

## 1 Introduction

Welded hollow spherical joints have become one of the widely used joint forms in the grid structure due to their simple connection method, reasonable force mechanism, and many other advantages [1]. Most space grid structures use anti-corrosion coatings to separate the metal surface from the environment, acting as a shield and protection. However, anti-corrosion treatment at the joints is more difficult, with an uneven thickness of the coating, leaving marks, brush patterns, and uneven color intensity, all creating the environment and conditions for corrosion. Corrosion, creep and other factors make the joint bearing capacity performance largely different from the design and will produce a significant capacity decline, especially in steel structures, which are prone to corrosion in a humid, corrosive environment with high air humidity and chloride ion content [2]. This corrosion phenomenon hurts large-span space steel structures, particularly their joint parts, making the strength, plasticity, and other mechanical indicators of structural members and joints significantly reduced [3–5], thus causing a few engineering accidents. The welded spherical joint grid structure of a machine repair workshop in Shanxi Province, China, collapsed, and the analysis of the cause of the accident found that the grid structure in the process of use, due to the lack of reasonable maintenance, the grid structure around the rods, joints and support at the obvious corrosion, resulted in a significant decrease in bearing capacity [6]. In a swimming pool in Chusovoy, Russia, the joints of a roofing grid were affected by the corrosive effect due to being in humid air for a long time and eventually collapsed [7]. The corrosion effect caused huge economic losses to the steel structure and had a serious impact on the safety performance of the structure [8].

At present, research on the corrosion of steel grids is mostly focused on materials [9–11] and members [12–17]. Liu et al. [18] conducted an experimental study of hollow spherical joints, and the results showed that the corrosion morphology of the joints consisted mainly of uniform

**Cite this article as:** Qiu, F., Wang, Y., Gao, Y., Zhang, Z., Qian, H., Wang, H., Fan, F. "Study of the Key Mechanical Properties of Welded Hollow Spherical Joints after Uniform Corrosion", Periodica Polytechnica Civil Engineering, 67(2), pp. 571–581, 2023. https://doi.org/10.3311/PPci.21006

corrosion with slight pitting corrosion. Zhao et al. [19] provided a method for the reinforcement of grid structures connected by welded hollow spherical joints and proposed a numerical method considering the degradation of connections to investigate the buckling capacity of a single-layer reticulated shell [20]. Some studies have also discussed the effect of size on the bearing capacity of welded hollow spherical joints [21–22].

The mechanical properties of building steel joints after corrosion are less researched and space steel structures using welded hollow spherical joint corrosion after the mechanical properties of research are even rarer. Guo et al. [23]proposed and investigated the method of strengthening welded hollow spherical joints. Stochastic analyses have been conducted by researchers to investigate the influence of the tension force on the probabilistic distribution of the bending capacity of welded hollow spherical joints [24]. As the part of the members to connect and contact, the joint is the most difficult corrosion treatment; thus, corrosion is most likely to occur (as in Figs. 1 and 2). Therefore, the study of the post-corrosion mechanical properties of welded hollow spherical joints becomes particularly important.

**Fig. 1** Corrosion of a welded hollow spherical joint

**Fig. 2** Corrosion in the joints in steel structures

Firstly, this paper established the FEM of a welded hollow spherical joint in one typical size with groove welds and a steel tube. Then, considering different uniform corrosion ratios of the welded hollow spherical joint, the simulations of three typical stresses on the welded hollow spherical joint in tension, compression, and bending were done. This paper gives a reference for the study of other sizes of welded hollow spherical joints and also provides a theoretical reference for understanding the post-corrosion mechanical properties and assessing structural safety.

## 2 Finite element model and analysis scheme

### 2.1 Refined finite element model

The welded hollow spherical joint finite element model is established with the ANSYS platform, using eight-joint SOLID185 units to simulate each component. The material of the sphere shell, steel tube, and drivepipe is Q235 steel, which is commonly used in building structures. The material properties of the groove weld are the same as those of the steel tube, and the strength is equal to that of the parent metal.

To obtain more accurate material information, the material properties of Q235 steel were tested by removing rectangular standard test materials 200 mm and 15 mm wide from the Q235 steel tube, as shown in Fig. 3.

The uniaxial tensile test was carried out by the relevant standards. The final yield strength was 281 MPa, and the ultimate strength was 378 MPa. The stress-strain curve obtained from the test is shown in Fig. 4. In this paper, the finite element simulation model is the multilinear kinematic hardening model. According to its stress-strain curve, the modulus of elasticity is taken as $2.06 \times 105$ N/mm$^2$, and Poisson's ratio is taken as 0.3.

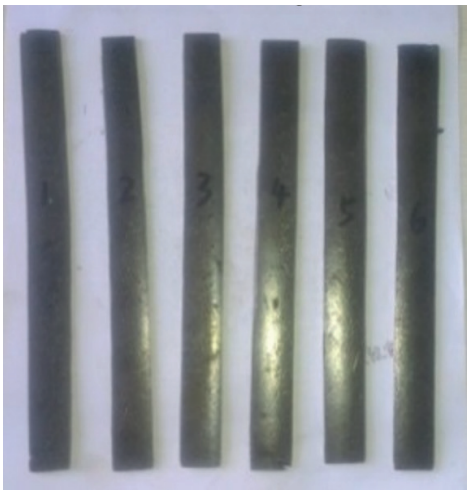

**Fig. 3** Standard test material of material properties test

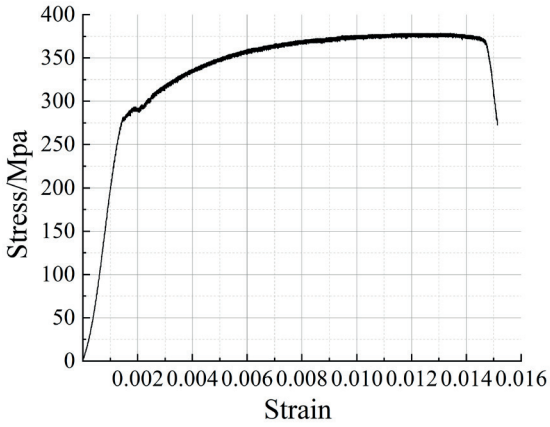


**Fig. 4** The stress-strain curve obtained from the material properties test

The existing analysis models of welded hollow spherical joints usually do not consider the weld and steel tube, which means they cannot simulate the influence of these two parts on the overall stiffness of the joints. To make the simulation results more accurate and in line with the actual situation, this paper selects one typical welded hollow spherical joint size according to the JGJ7-2010 Technical Specification for Space Frame Structures [25] (Fig. 5) to refine the joint connection part, as shown in Fig. 6. The final refined model of welded hollow spherical joints is shown in Fig. 7 and the size of FEM is shown in Table 1.

### 2.2 Corrosion simulation method

Existing relevant studies show that the load capacity is reduced when corrosion occurs at the surface of the welded hollow spherical joint [26] and it is in the most unfavorable state when the entire surface is corroded [27]. This study simulated the uniform corrosion occurring at the whole sphere shell surface.

Considering the corroded part cannot bear the loads, the element birth and death technique is used to deal with the FEM elements of the corroded part of the sphere shell, which means deactivating corrosion elements by multiplying their stiffness by a severe reduction factor [28]. The element birth and death technique makes the FEM obtain uniform corrosion of specified thickness (Fig. 8) and does not affect the mesh quality of the elements, which means good convergence.

### 2.3 Load simulation method

The simulated joints are loaded by displacement (as in Fig. 9) control in tension, compression, and bending, in which the joints are loaded in tension with 0.05 mm per step to apply upward displacement along the vertical direction at the top section joint of the model; the joints

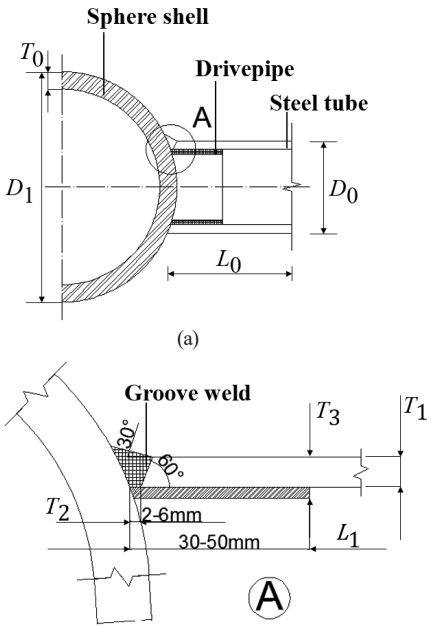


**Fig. 5** The connection requirement given by [25]: (a) Sphere shell, Drivepipe, and Steel tube, (b) Groove weld

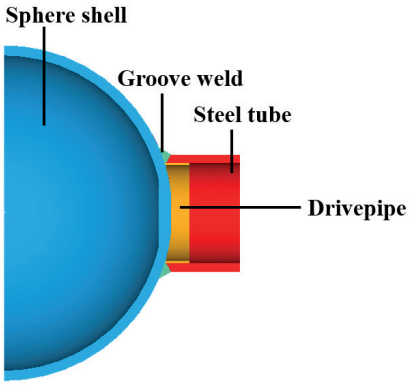


**Fig. 6** The sectional drawing of refined FEM

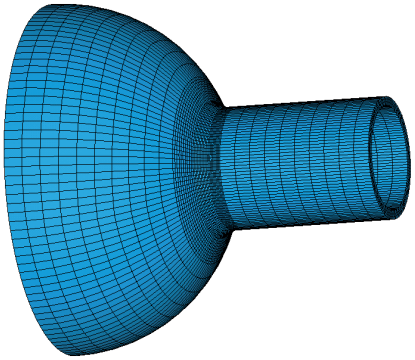

**Fig. 7** Refined FEM based on [26]

**Table 1** The size of the welded hollow spherical joint

| $D_0$/mm | $D_1$/mm | $L_0$/mm | $L_1$/mm | $T_0$/mm | $T_1$/mm | $T_2$/mm | $T_3$/mm |
|---|---|---|---|---|---|---|---|
| 80 | 200 | 100 | 30 | 12 | 10 | 3 | 2 |

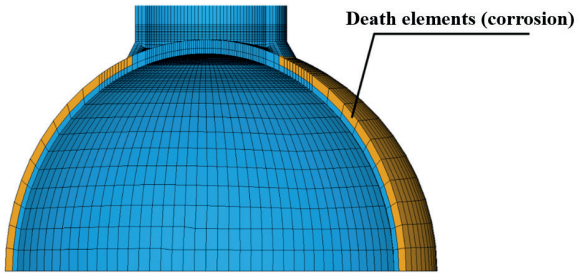


**Fig. 8** Uniform corrosion based on the element birth and death technique

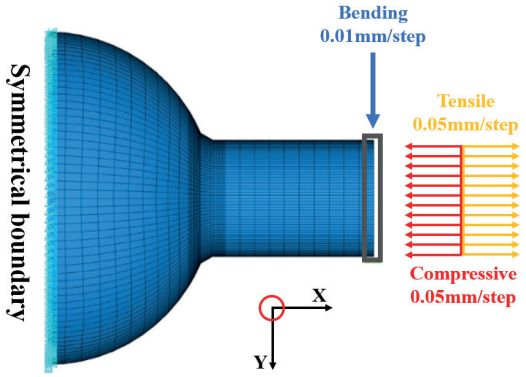


**Fig. 9** The method of FEM to simulate tension, compression, and bending

are loaded in compression with 0.05 mm per step to apply downward displacement along the vertical direction at the top section joint of the model; the joints are loaded in bending with 0.1 mm per step to apply displacement along the vertical direction at the top section joint of the model along the lateral direction.

### 2.4 Analysis scheme

The analysis scheme is shown in Table 2, and uniform corrosion occurs at the whole sphere shell surface.

For the convenience of expression, each corrosion FEM by the L-R method is named, where L is the method of loads and R is the uniform corrosion sphere shell thickness as a ratio of the original sphere shell thickness. For example, the T-0.3 is the FEM that is tensioned and has a thickness that after corrosion is 8.4 mm of sphere shell. To give the influence law of uniform corrosion depth on the mechanical properties of welded hollow spherical joints, the ratio of uniform corrosion thickness is the independent variable control index.

## 3 Analysis of tensile properties

The axial force is the most common form of force in space structures. The tensile performance of the joint after uniform corrosion is first analyzed.

### 3.1 Analysis of failure mode

The limit state stress cloud diagram of the joint FEM in tension after corrosion is shown in Fig. 10. As the corrosion depth increases, the joint has two successive tensile

**Table 2** The analysis scheme

| Method of loads | The ratio of corrosion depth |
|---|---|
| T (tension) | 0,0.1,0.2,0.3,0.4,0.5 |
| C (compression) | 0,0.1,0.2,0.3,0.4,0.5 |
| B (bending) | 0,0.1,0.2,0.3,0.4,0.5 |

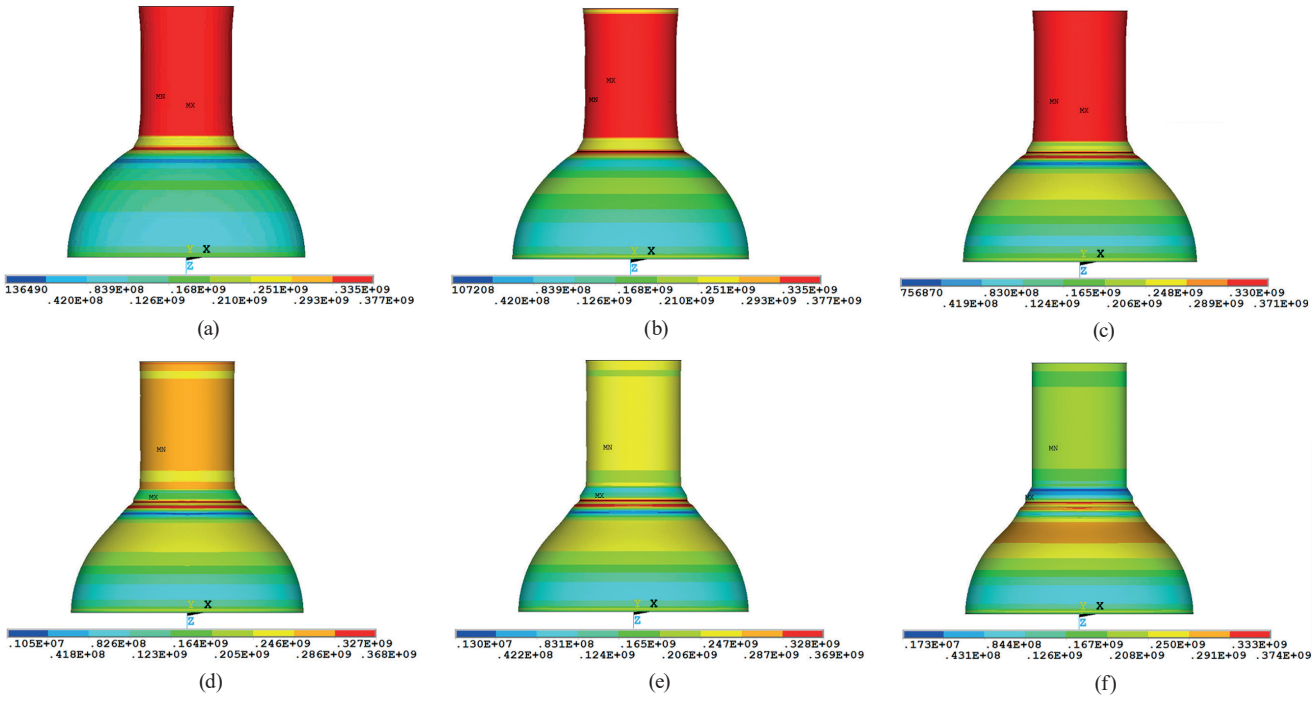


**Fig. 10** The limit states stress cloud diagram of the joint under tension after corrosion: (a) T-0, (b) T-0.1, (c) T-0.2, (d) T-0.3, (e) T-0.4, (f) T-0.5

failure modes: corrosion depth below 0.2 of the original thickness of the sphere shell, the steel tube components are the first to reach the ultimate tensile strength and failure, with the corrosion depth increases, the sphere shell has no obvious deformation and stress gradually rise; corrosion depth of more than 0.2 of the original thickness of sphere shell, the sphere shell plastic deformation becomes obvious, the yield area gradually increased, the weld and sphere shell connection parts to reach the ultimate tensile strength and make the joint failure. Table 3 shows the different corrosion depths of the sphere shell and the corresponding tensile capacity of the joint.

### 3.2 Load-displacement curve

Fig. 11 gives the load-displacement curve of joints after corrosion under tension with different corrosion depths of the sphere shell, it can be seen that corresponding to its failure mode, with different sphere shell corrosion depths, welded hollow spherical joints under tension load-displacement curve in two forms: the first form of corrosion depth of less than 0.2 of the original thickness of sphere shell, the joint initial stiffness and ultimate tensile capacity unchanged; the second form of corrosion depth of more than 0.2 of the original thickness of sphere shell, the joint initial stiffness, and ultimate tensile capacity gradually decreases with the corrosion depth of sphere shell increase.

### 3.3 Tensile capacity degradation analysis

To better obtain the influence of the corrosion depth on the joint tensile capacity, linear fitting is performed to process the tensile capacity and corrosion depth of the data. The calculation method of related parameters is as follows:

$$x = d_c / d_0 , \tag{1}$$

$$y_t = f_{T,d_c} / f_T . \tag{2}$$

The equation of linear fitting results is:

**Table 3** Tensile capacities of different FEMs

| Uniform corrosion depth ratio of sphere shell | Ultimate tensile capacity/kN |
|---|---|
| 0 | 358.22 |
| 0.1 | 359.69 |
| 0.2 | 351.46 |
| 0.3 | 298.5 |
| 0.4 | 252.14 |
| 0.5 | 215.86 |

$$\begin{cases} y_t = 1.0020518 & , \ x < 0.1743 \\ y_t = -1.26034x + 1.2217297 & , \ x \geq 0.1743 \end{cases}, \tag{3}$$

where $d_c$ is the thickness of the sphere shell after corrosion. $d_0$ is the thickness of the original sphere. $f_{T,d_c}$ is the tensile capacity of the joint when the thickness of the sphere shell is $d_c$. $f_T$ is the tensile capacity of the joint when the thickness of the sphere shell is $d_0$.

According to Eq. (3), the failure mode will alter when $x \geq 0.1743$. Fig. 12 shows the linear fitting results, and the vertical red line in Fig. 12 indicates the failure mode conversion dividing line.

From the linear fitting results, the analysis shows that the $x$ is 0.1743 below, the joint tensile capacity is determined by the steel tube and remains unchanged, so the curve remains fairly flat, and the limit state performance is steel tube failure. When the $x$ reaches 0.1743 above, the joint tensile capacity begins to reduce, and its reduced

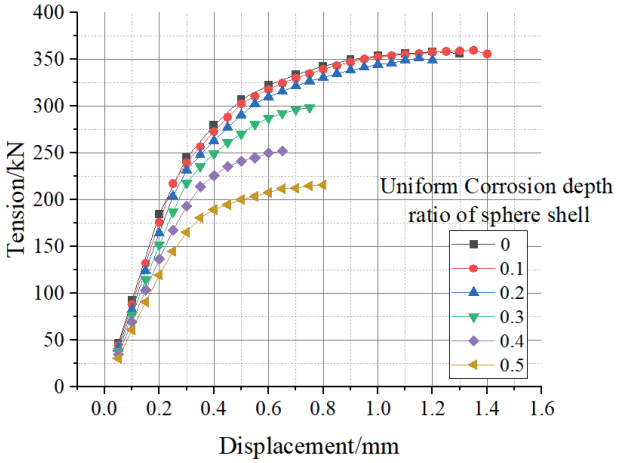


**Fig. 11** The load–displacement curve of joints after corrosion under tension with different corrosion depths of the sphere shell

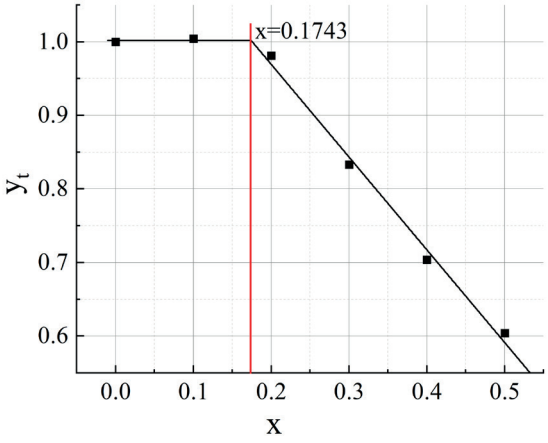


**Fig. 12** The linear fitting results of FEM under tension

level has an obvious linear relationship with the sphere shell corrosion depth. The corrosion depth of each 10% increases, the joint tensile capacity decreases by approximately 12.6% on average, and the limit state performance is sphere shell failure.

## 4 Compressive performance analysis

In addition to examining the effect of corrosion on the tensile properties of the joints, the effect of uniform corrosion on the compressive properties of the joint is also simulated.

### 4.1 Failure mode analysis

The limit state stress cloud diagrams of the joint FEM in compression after corrosion are shown in Fig. 13. Analysis shows that as the corrosion depth increases, the joint has two successive compression failure modes: corrosion depth below 0.2 of the original thickness of the sphere shell, the steel tube components are the first to reach the ultimate compressive strength and failure, with the corrosion depth increasing, the sphere shell has no obvious deformation and stress gradually rising; corrosion depth of more than 0.2 of the original thickness of the sphere shell, the sphere shell plastic deformation is obvious, the yield area gradually increases, and its weld and sphere shell connection parts reach the ultimate compressive strength and make the joint compression buckling failure. Table 4 shows the different corrosion depths of spherical shells and the corresponding compressive capacity of the joint.

Compared to failure modes under tension and compression when the ratio of corrosion depth is more than 0.2, the sphere shell buckles near the connection between the sphere shell and tube when the load is compression so the failure mode is referred to as instability failure (Fig. 14(a)). While under tension the sphere shell plastic deformation becomes obvious (Fig.14(b)), which means the failure mode is referred to as plastic failure. Although when the corrosion depth ratio is less than 0.2 the failure modes are both the steel tube plastic deformation, the deformation of the two loading cases is not the same as well (Fig. 15).

**Table 4** The compressive capacities of different FEMs

| Uniform corrosion depth ratio of sphere shell | Ultimate compressive capacity/kN |
|---|---|
| 0 | 358.66 |
| 0.1 | 359.66 |
| 0.2 | 351.48 |
| 0.3 | 298.74 |
| 0.4 | 253.38 |
| 0.5 | 216.42 |

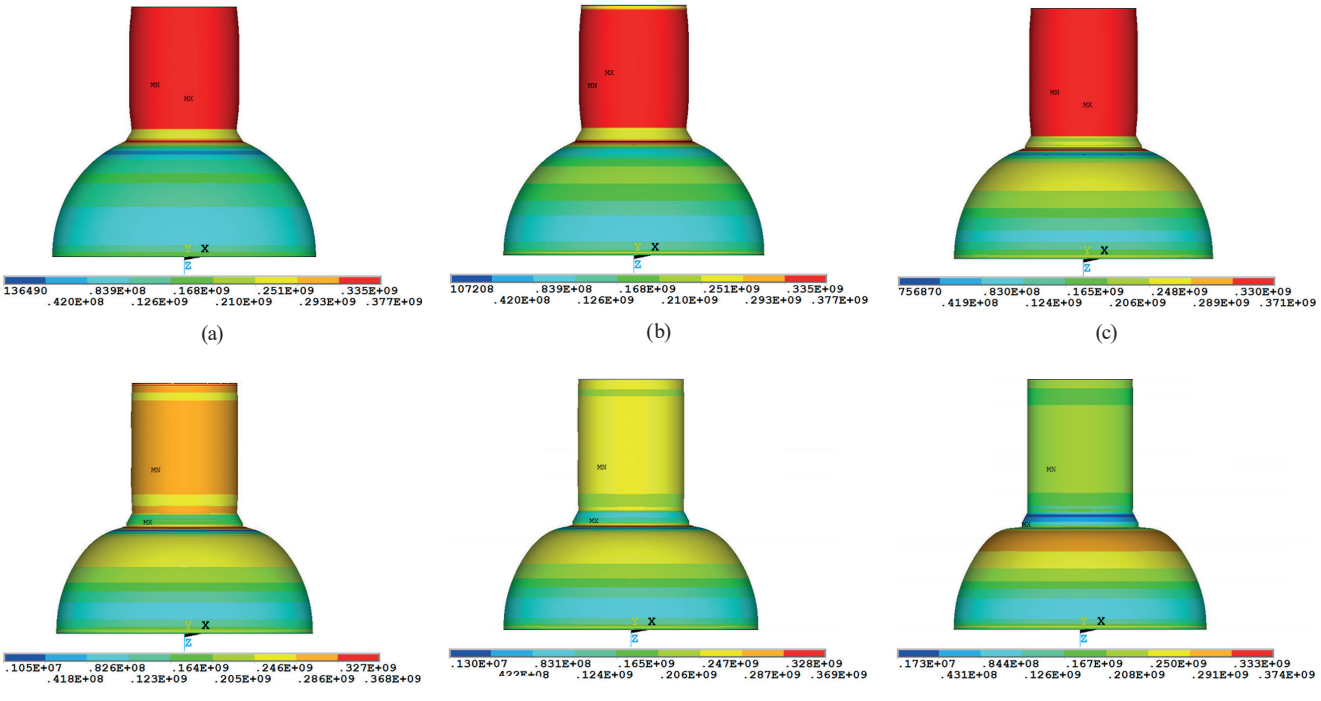


**Fig. 13** The limit states stress cloud diagram of the joint under compression after corrosion: (a) C-0, (b) C-0.1, (c) C-0.2, (d) C-0.3, (e) C-0.4, (f) C-0.5

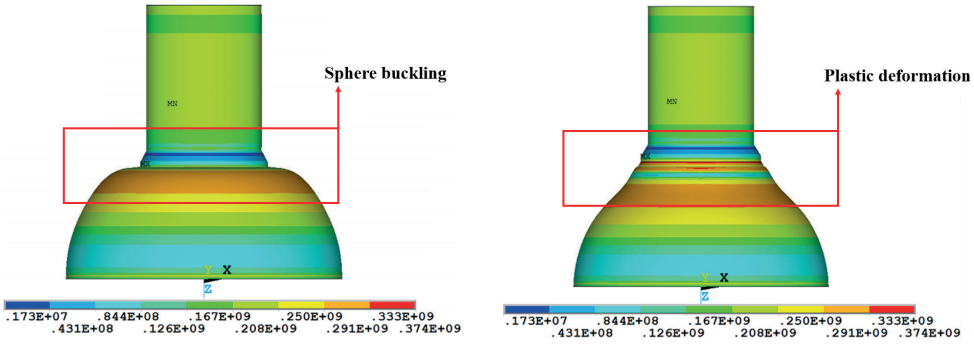


(a) (b)

**Fig. 14** The ultimate stress cloud diagrams when the corrosion depth ratio is 0.5: (a) under compression, (b) under tension

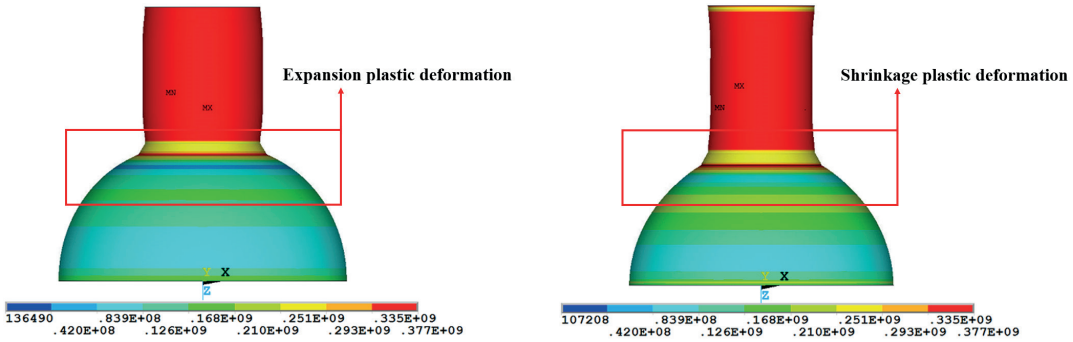


(a) (b)

**Fig. 15** The ultimate stress cloud diagrams when the corrosion depth ratio is 0.1: (a) under compression, (b) under tension

### 4.2 Load-displacement curve

Fig. 16 gives the load-displacement curve of the joint after corrosion under pressure. It can be seen that corresponding to its failure mode, with different corrosion depths, welded hollow spherical joints under compression load-displacement curve in two forms: the first form of corrosion depth of less than 0.2 of the original thickness of sphere shell, the joint initial stiffness and ultimate load capacity unchanged;

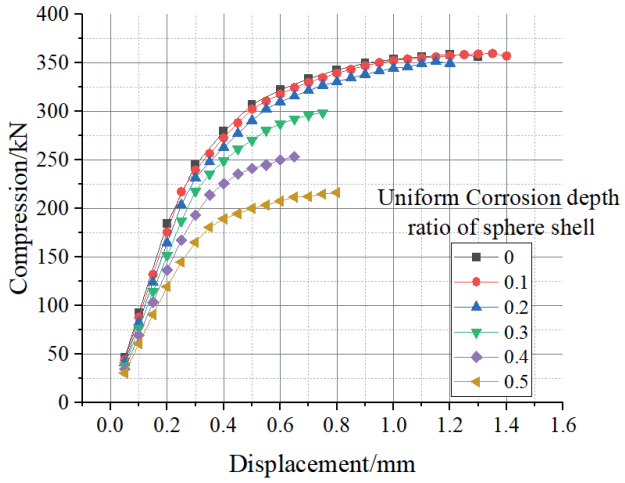


**Fig. 16** The load-displacement curve of joints after corrosion under compression with different corrosion depths of the sphere shell

the second form of corrosion depth of more than 0.2 of the original thickness of sphere shell, the joint initial stiffness, and ultimate compressive capacity gradually decrease with the corrosion depth of sphere shell increase.

### 4.3 Compressive capacity degradation analysis

To better obtain the influence of corrosion depth on the joint compressive capacity, linear fitting is taken to process the tensile capacity and corrosion depth of the data. The calculation method of related parameters is as follows:

$$y_c = f_{C,d_c} / f_C . \tag{4}$$

The equation of linear fitting results is:

$$\begin{cases} y_c = 1.0013941 + & ,x < 0.1743 \\ y_c = -1.2618x + 1.2203591 & ,x \geq 0.1743 \end{cases}, \tag{5}$$

where $f_{C,d_c}$ is the compressive capacity of the joint when the thickness of the sphere shell is $d_c$. $f_C$ is the compressive capacity of the joint when the thickness of the sphere shell is $d_0$.

According to Eq. (5), the failure mode will alter when $x \geq 0.1743$. Fig. 17 shows the linear fitting results, and the vertical black line in Fig. 17 indicates the failure mode conversion dividing line.

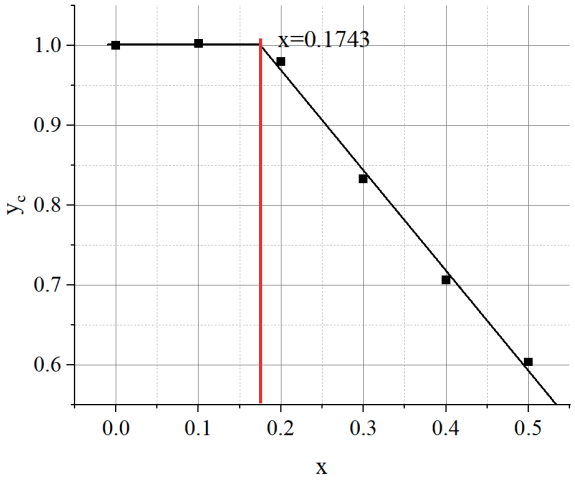


**Fig. 17** The linear fitting results of FEM under compression

From the linear fitting results, the analysis shows that when the $x$ is 0.1743 below, the joint compressive capacity is determined by the steel tube and remains unchanged, so the curve remains flat, and the limit state performance is steel tube failure. When the $x$ reaches 0.1743 above, the joint compressive capacity begins to reduce, and its reduced level has an obvious linear relationship with the sphere shell corrosion depth. The corrosion depth of each 10% increases, the joint compressive capacity decreases by approximately 12.56% on average, and the limit state performance is sphere shell compression buckling failure.

## 5 Bending performance analysis

Welded hollow spherical joints are often used in single-layer reticulated shell structures, which means that the bending performance of the joints is also particularly important, so this performance after uniform corrosion is simulated.

### 5.1 Analysis of failure mode

The limit state stress cloud diagrams of the joint FEM in bending after corrosion are shown in Fig. 18. The analysis shows that when the joint transerves bending, the steel tube reaches the ultimate bending strength and failure. As the corrosion depth increases, the steel tube stress decreases significantly. At the same time, part of the area of the sphere shell that is perpendicular to the direction of bending has 0 stress; as the corrosion depth increases, the 0 stress area gradually decreases, and the overall increase in sphere shell stress. In the weld near the sphere shell, the yield area gradually increases, and the bearing capacity of the joint reduces.

It can be seen that corrosion on the joint bending capacity of the impact is not like tensile and compressive capacity exists more obvious boundary, but with the corrosion, depth increases, the connection yield area gradually increased, so that the joint bearing capacity and then decreased. The sphere shell near the weld part reaches

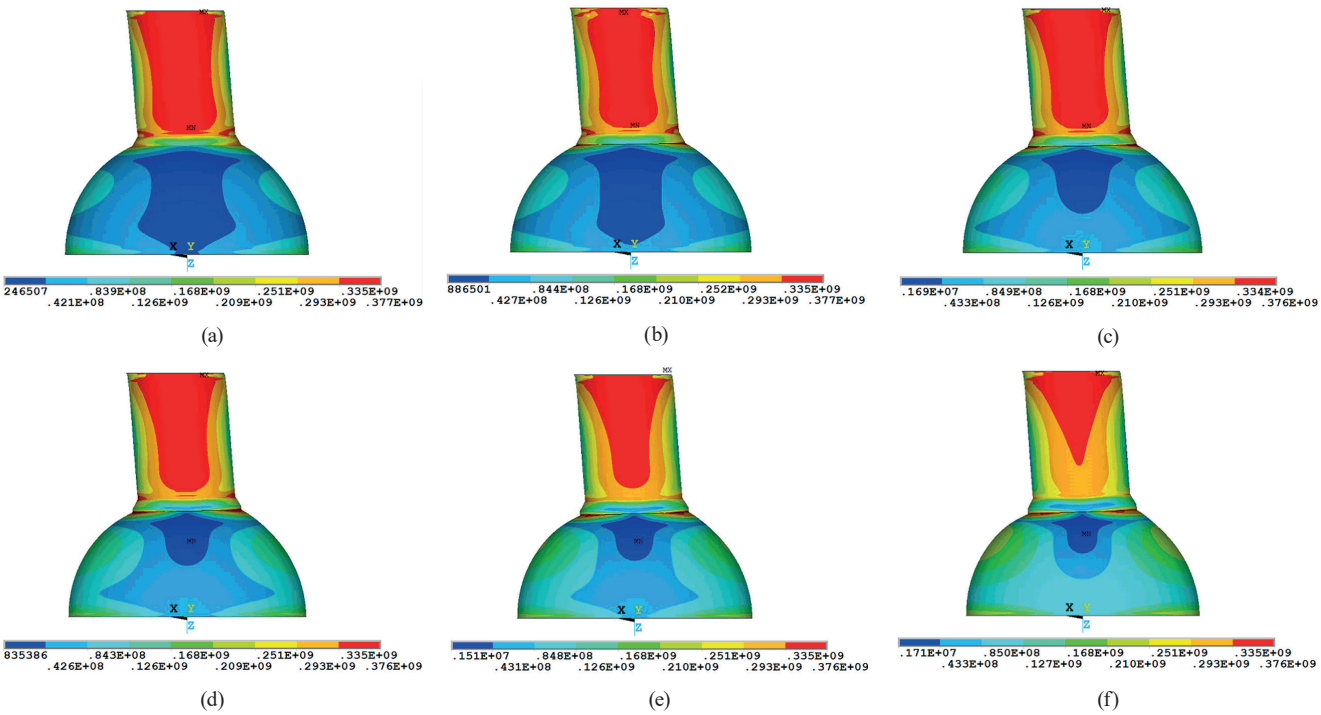


**Fig. 18** The limit states stress cloud diagram of the joint under bending after corrosion: (a) B-0, (b) B-0.1, (c) B-0.2, (d) B-0.3, (e) B-0.4, (f) B-0.5

the ultimate bending capacity and failure. Table 5 shows the joint sphere shell parts of different uniform corrosion depths and the corresponding bending capacity.

### 5.2 Load-displacement curve

Fig. 19 gives the load-displacement curve when the joint after corrosion is under pressure. As the corrosion depth increases, the initial stiffness of the joint does not change much, the ultimate bending capacity gradually decreases in correspondence with the failure mode, and the ultimate bending capacity decreases faster when the corrosion depth is greater than 0.3 of the original thickness of the sphere shell and decreases by approximately 20% when the corrosion depth reaches 0.5 of the original thickness of the sphere shell.

### 5.3 Bending capacity degradation analysis

To better obtain the influence of corrosion depth on the joint bending capacity, the use of a secondary curve fitting way to the bearing capacity and corrosion depth of data processing. The calculation method of related parameters is as follows:

$$y_b = M_{d_c} / M_0 . \tag{6}$$

The equation of secondary curve fitting is:

$$y_b = -0.00716x^2 - 0.03276x + 0.9958386 , \tag{7}$$

where $M_{d_c}$ is the bending capacity of the joint when the thickness of the sphere shell is $d_c$. $M_C$ is the bending capacity of the joint when the thickness of the sphere shell is $d_0$.

Fig. 20 shows the secondary curve fitting results. Analysis shows that at each corrosion depth, the joint bending bearing capacity after corrosion is always lower than the capacity without corrosion, and the limit state is performed as a joint bending failure. The bending capacity reduction level and corrosion depth have an obvious quadratic curve relationship: as the depth of corrosion increases, the joint bearing capacity decline rate gradually accelerates.

**Table 5** The bending capacities of different FEMs

| Uniform corrosion depth ratio of sphere shell | Ultimate bending capacity/ (kN·m) |
|---|---|
| 0 | 1.6521 |
| 0.1 | 1.6168 |
| 0.2 | 1.5824 |
| 0.3 | 1.535 |
| 0.4 | 1.4339 |
| 0.5 | 1.3195 |

## 6 Conclusions

This paper establishes a refined finite element model of one commonly used size welded hollow spherical joint based on the specification [25], which can consider the effects of uniform corrosion, and analyzes its typical stress state. It is worth noticing, the compressive and tensile capacities in results are close to each other. In fact, the compressive capacity can be affected by the size parameters of welded hollow spherical joints such as the thickness [21] and diameter [22] of the hollow spheres. More different sizes of welded hollow spherical joints are worth to be studied. The following conclusions are drawn based on the study of this paper.

(1) The joint under tension has two modes of failure: the first mode is when the corrosion depth is lower than 17.43%, the steel tube is the first to reach the ultimate tension capacity and failure, and the joint's initial stiffness and ultimate tension capacity are unchanged; the second

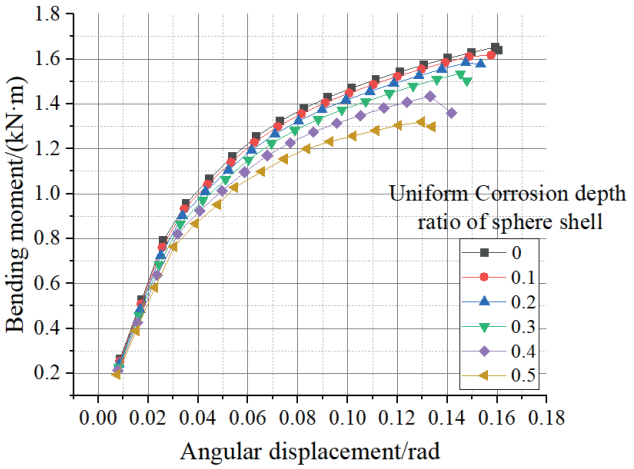


**Fig. 19** The load–displacement curve of joints after corrosion under bending with different corrosion depths of the sphere shell

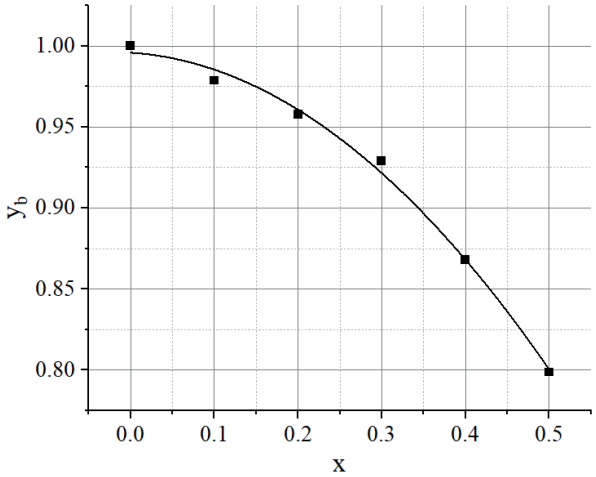


**Fig. 20** The secondary curve fitting of FEM under bending

mode is the corrosion depth of more than 17.43%, the joint weld and spherical shell connection part to reach the ultimate tensile capacity and plastic deformation occurs to make the joint failure, so the failure mode is referred to as plastic failure. Its initial stiffness with the corrosion depth increases gradually reduce. In this situation, the ultimate tensile capacity reduction level and corrosion depth have an obvious linear relationship.

(2) The joint under compression has two failure modes: the first mode is when the corrosion depth is lower than 17.43%, the steel tube is the first to reach the ultimate compression capacity and failure, and the joint's initial stiffness and ultimate compression capacity are unchanged; the second mode is the corrosion depth of more than 17.43%, the joint weld and sphere shell connection part to reach the ultimate compressive strength and the failure mode is the sphere shell buckles near the connection between the sphere shell and tube, so the failure mode is referred to as instability failure. Its initial stiffness with corrosion depth increases gradually decreases. In this situation, the ultimate compression capacity reduction level and corrosion depth also have an obvious linear relationship.

(3) The joint under the bending action at each corrosion depth has a sphere shell close to the weld part to reach the ultimate bending capacity and undergo joint bending failure. The joint initial stiffness change is small, and the ultimate bending capacity and corrosion depth have a quadratic curve relationship. Unlike the other two capacities, the bending capacity of the joint will decrease immediately when uniform corrosion occurs.

**Acknowledgment**

This work was supported by the National Natural Science Foundation of China (Grant No. 51308154) and partially supported by The Science and Technology Development Program of Weihai (Grant No. 2016DXGJMS03) and the National Key Research and Development Program (Grant No. 2016YFC0802003).

## References

[1] Zhao, Z., Liu, H., B, Liang, B. "Assessment of the bending capacity of welded hollow spherical joints with pit corrosion", Thin-Walled Structures, 131, pp. 274–285, 2018. https://doi.org/10.1016/j.tws.2018.07.010

[2] Hirokawa, H., Yoshikawa, M., Tamara, A., Hashimoto, M. "A Proposal on Corrosion Protective Measures of Coastal Steel Structures for Super-Long Service Life", Steel Construction Engineering, 12(47), pp. 1–9, 2005. https://doi.org/10.11273/jssc1994.12.47_1

[3] Sultana, S., Wang, Y., Sobey, A. J., Wharton, J. A., Shenoi, R. A. "Influence of corrosion on the ultimate compressive strength of steel plates and stiffened panels", Thin-Walled Structures, 96, pp. 95–104, 2015. https://doi.org/10.1016/j.tws.2015.08.006

[4] Albrecht, P., Hall Jr., T. T. "Atmospheric Corrosion Resistance of Structural Steels", Journal of Materials in Civil Engineering, 15(1), pp. 2–24, 2003. https://doi.org/10.1061/(ASCE)0899-1561(2003)15:1(2)

[5] Dobruchowska, E., Gilewicz, A., Warcholinski, B., Libralesso, L., Batory, D., Szparaga, L., Murzynski, D., Ratajski, J. "Al-Mn based coatings deposited by cathodic arc evaporation for corrosion protection of AISI 4140 alloy steel", Surface and Coatings Technology, 362, pp. 345–354, 2019. https://doi.org/10.1016/j.surfcoat.2019.02.014

[6] Luan, G. "The collapse accident analysis of a welding hollow ball grid workshop", MSc Thesis, Taiyuan University of Technology, 2014. (in Chinese) https://doi.org/10.7666/d.Y2692481

[7] Lei, H. "Steel structure accident analysis and treatment", China Building Materials Industry Press, 2003. ISBN 7-80159-386-3 (in Chinese)

[8] Liu, X., Hou, P., Zhao, X., Ma, X., Hou, B. "The polyaniline-modified TiO2 composites in water-based epoxy coating for corrosion protection of Q235 steel", Journal of Coatings Technology and Research, 16(1), pp. 71–80, 2019. https://doi.org/10.1007/s11998-018-0101-4

[9] Sun, J., Ding, Z., Huang, Q. "Corrosion fatigue life prediction for steel bar in concrete based on fatigue crack propagation and equivalent initial flaw size", Construction and Building Materials, 195, pp. 208–217, 2019. https://doi.org/10.1016/j.conbuildmat.2018.11.056

[10] Hájková, K., Šmilauer, V., Jendele, L., Červenka, J. "Prediction of reinforcement corrosion due to chloride ingress and its effects on serviceability", Engineering Structures, 174, pp. 768–777, 2018. https://doi.org/10.1016/j.engstruct.2018.08.006

[11] Qin, S., Cui, W. "Effect of corrosion models on the time-dependent reliability of steel plated elements", Marine Structures, 16(1), pp. 15–34, 2003. https://doi.org/10.1016/S0951-8339(02)00028-X

[12] Bergman, R. M., Levitsky, S. P., Haddad, J., Gutman, E. M. "Stability loss of thin-walled cylindrical tubes, subjected to longitudinal compressive forces and external corrosion", Thin-Walled Structures, 44(7), pp. 726–729, 2006. https://doi.org/10.1016/j.tws.2006.08.006

[13] Sargand, S. M., Khoury, I., Hussein, H. H., Masada, T. "Load Capacity of Corrugated Steel Pipe with Extreme Corrosion under Shallow Cover", Journal of Performance of Constructed Facilities, 32(4), 04018050, 2018. https://doi.org/10.1061/(ASCE)CF.1943-5509.0001196

[14] Wang, R., Ajit Shenoi, R., Sobey, A. "Ultimate strength assessment of plated steel structures with random pitting corrosion damage", Journal of Constructional Steel Research, 143, pp. 331–342, 2018. https://doi.org/10.1016/j.jcsr.2018.01.014

[15] Oszvald, K., Dunai, L. "Behaviour of corroded steel angle compression members – numerical study", Periodica Polytechnica Civil Engineering, 57(1), pp. 63–75, 2013. https://doi.org/10.3311/PPci.2142

[16] Oszvald, K., Dunai, L. "Effect of corrosion on the buckling of steel angle members - experimental study", Periodica Polytechnica Civil Engineering, 56(2), pp. 175–183, 2012. https://doi.org/10.3311/pp.ci.2012-2.04

[17] Li, J., Li, M., Huang, X., Hao, F., Rui, X., Zhang, Y. "Crosspoint Localization of Spiral and Girth Welds of Spiral Steel Pipelines", IEEE Access, 8, pp. 160387–160395, 2020. https://doi.org/https://doi.org/10.1109/ACCESS.2020.3020793

[18] Liu, H., Chen, H., Chen, Z. "Residual behavihour of welded hollow spherical joints under corrosion and de-rusting", Journal of Constructional Steel Research, 167, 105977, 2020. https://doi.org/10.1016/j.jcsr.2020.105977

[19] Zhao, Z., Gao, T., Gao, H., Zhang, P., Jian, X. "Compression behavior of randomly corroded welded hollow spherical joints reinforced by different methods", Engineering Failure Analysis, 136, 106201, 2022. https://doi.org/10.1016/j.engfailanal.2022.106201

[20] Zhao, Z., Li, T., Yang, Y., Zhang, Z., Zhang, N. "Method for considering corroded joints in buckling analysis of single-layer reticulated shell structures", Mechanics of Advanced Materials and Structures, 29(28), pp. 7732–7742, 2022. https://doi.org/10.1080/15376494.2021.2006834

[21] Liu, H., Ying, J., Chen, Z., Zhou, Y., Yan, X. "Ultimate tensile and compressive performances of welded hollow spherical joints with H-beam", Journal of Constructional Steel Research, 150, pp 195–208, 2018. https://doi.org/10.1016/j.jcsr.2018.08.018

[22] Yan, X., Duan, Y., Zhang, Y., Chen, Z., Zhang, Q. "Study on compressive bearing capacity and axial stiffness of welded hollow spherical joints with H-shaped steel member", Engineering Structures, 203, 109821, 2020. https://doi.org/10.1016/j.engstruct.2019.109821

[23] Guo, Z., Xu, X., Du, Y., Chen, Y. "Behaviors of welded hollow spherical joints strengthened by unidirectional annular ribs", Structures, 30, pp. 11–24, 2021. https://doi.org/10.1016/j.istruc.2020.12.080

[24] Zhao, Z., Dai, B., Xu, H., Li, T. "Bending capacity of corroded welded hollow spherical joints with considering interaction of tension force and bending moment", Structures, 34, pp. 2656–2664, 2021. https://doi.org/10.1016/j.istruc.2021.09.042

[25] Industry Standard of the PRC "JGJ7-7-2010 Technical specification for space frame structures", Ministry of Housing and Urban–Rural Development, Peking, China, 2010.

[26] Zhao, Z., Liu, H., Liang, B. "Compressive Capacity of Corroded Welded Hollow Spherical Joints", Journal of Performance of Constructed Facilities, 33(1), 04018094, 2019. https://doi.org/10.1061/(ASCE)CF.1943-5509.0001247

[27] Zhao, Z., Liu, H., Liang, B. "Bending capacity of corroded welded hollow spherical joints", Thin-Walled Structures, 127, pp. 523–539, 2018. https://doi.org/10.1016/j.tws.2018.03.007.

[28] Ansys "Advanced Analysis Guide, 8.2., Understanding Element Birth and Death", [online] Available at: www.ansys.com [Accessed: 1 August 2022]